

Accelerating the variational quantum eigensolver using parallelism

Lana Mineh^{1,*} and Ashley Montanaro^{1,2}

¹*Phasecraft Ltd.*

²*School of Mathematics, University of Bristol*

(Dated: May 10, 2023)

Quantum computers are getting larger and larger, but device fidelities may not be able to keep up with the increase in qubit numbers. One way to make use of a large device that has a limited gate depth is to run many small circuits simultaneously. In this paper we detail our investigations into running circuits in parallel on the Rigetti Aspen-M-1 device. We run two-qubit circuits in parallel to solve a simple instance of the Hubbard model using the variational quantum eigensolver. We present results for running up to 33 circuits in parallel (66 qubits), showing that with the use of error mitigation techniques it is possible to make use of, and gain a real-time speedup from, parallelisation on current quantum hardware. We obtain a speedup by 18× for exploring the VQE energy landscape, and by more than 8× for running VQE optimisation.

Quantum computers in the coming years are expected to have thousands of qubits, but it is likely that the fidelity of devices will still restrict the ability to do large computations involving many qubits. One possible way to make better use of a device is to run multiple smaller computations in parallel, increasing the speed of the overall algorithm being run. Noisy intermediate-scale quantum (NISQ) algorithms and hybrid quantum-classical algorithms such as the variational quantum eigensolver (VQE) [1, 2] naturally lend themselves to parallelism, and are natural test cases for the ability of quantum computers to take advantage of this concept.

A number of works have investigated the theory and implementation of parallelism (also called multi-programming) on NISQ devices. Algorithms have been proposed that partition chips into regions of reliable qubits, allowing for circuits of different depths and size to be run simultaneously [3–6]. On cloud systems, this could potentially allow multiple users to execute circuits on the same chip at the same time, increasing the throughput of quantum devices. Demonstrations of the VQE algorithm in parallel have also been performed for two-qubit deuteron and molecular hydrogen, in particular executing circuits to measure all of the Pauli terms in a Hamiltonian simultaneously [4, 6].

These last works introduce and demonstrate the use of techniques for achieving a speedup by parallelism. For example, in [6], up to 24 circuits are run in parallel (via 12 VQE parameters and 2 measurement settings), implying a speedup by up to 24 times. However, it is important to note that running circuits in parallel on a quantum computer does not immediately imply a faster or more accurate algorithm. Given the need to access quantum hardware via the cloud, network latency and the need to transmit additional data might wipe out any speedup obtained from parallelism. This is especially relevant to VQE algorithms, which have an inherently sequential flavour and require many round-trips between the

classical and quantum computer. Indeed, we find below that the choice of which algorithm to use for VQE has crucial implications for the level of speedup via parallelism that can be achieved. Also, crosstalk and the use of lower-fidelity qubits might reduce the accuracy of parallel algorithms [3, 4].

In this paper, we go into more depth regarding the use of parallelism within variational quantum algorithms, with the aim of making efficient use of near-term quantum hardware, and accelerating actual running times of algorithms. To do this we conduct a detailed investigation of one simple case of VQE on Rigetti hardware – solving the compressed two-site half-filled Hubbard model, which maps to a two-qubit circuit. This exact problem has previously been investigated on quantum hardware using Rigetti Aspen-4 and Aspen-7 [7]. Here, we demonstrate that a wall-clock time speedup can indeed be obtained for VQE: by a factor of more than 8 for the optimisation process (when using the BayesMGD optimisation algorithm [8]), and by a factor of 18 for exploring the VQE landscape.

In Section I, we discuss the details of the problem that we solve on the quantum computer. We lay out the particulars of the VQE algorithm, from the ansatz circuit and classical optimisers to the way in which parallelism is incorporated into the algorithm. In Section II we present the experimental results from Rigetti’s 80-qubit Aspen-M-1 device, where we run up to 33 circuits in parallel (66 qubits). From benchmarking in Section II A we find that as we add more circuits in parallel, the average error in the circuits gets worse but is somewhat mitigated through the use of error correction techniques. In Section II B we carry out the full VQE optimisation procedure using different parallelisation techniques and classical optimisers, finding that best use of the device is made when running circuits with different variational parameters and using a classical optimiser that can best make use of batch circuit runs. We conclude in Section III that this could open the way for using parallelisation within the VQE algorithm to carry out rough calculations, using the results to inform a more accurate run on one circuit. This could reduce the required running time of

* lana@phasecraft.io

variational algorithms on NISQ devices.

I. OUTLINING THE PROBLEM

The Hubbard model [9] is one of the simplest models of interacting electrons on a lattice, making it a good target for NISQ devices. Despite decades of research, a full description of the 2D model beyond approximations is still an open problem [10], and is thought to be relevant to applications such as high-temperature superconductivity [11].

In this paper, we will concern ourselves with solving the half-filled 2×1 Hubbard model for $t = 1$, $U = 2$; a case which has previously been investigated thoroughly on Rigetti hardware [7]. Using the Jordan-Wigner transform, the 2×1 model would map onto four qubits. However, we will make use of the compressed representation outlined in [7] which allows us to map the Hamiltonian onto two qubits. The compressed Hubbard Hamiltonian on two sites is now as follows:

$$H_C = -t(X \otimes I + I \otimes X) + \frac{U}{2}(I + Z \otimes Z) \quad (1)$$

$$= H_{\text{hop}} + H_{\text{os}} = \begin{pmatrix} U & -t & -t & 0 \\ -t & 0 & 0 & -t \\ -t & 0 & 0 & -t \\ 0 & -t & -t & U \end{pmatrix},$$

where t is the tunnelling amplitude (which governs the hopping term) and U is the Coulomb potential (which governs the onsite term).

We will aim to produce the ground state of this Hamiltonian using the VQE algorithm. This works by preparing a parameterised ansatz circuit $|\psi(\theta)\rangle$ on the quantum computer and using the classical computer to optimise the circuit with the aim of minimising $\langle\psi(\theta)|H_C|\psi(\theta)\rangle$.

There are a number of different ways in which we could make use of parallelism in the VQE algorithm. Let p be the number of VQE circuits run in parallel on the same quantum device.

- The same VQE circuit (with the same variational parameters) could be run in parallel. Compared to standard VQE, this generates $p \times$ more shots to estimate the energy with every run of the quantum computer. This has the potential to reduce the running time of the algorithm as the desired number of shots could be reached earlier, or increase the accuracy of the solution in the same running time as standard VQE.
- Each parallel circuit could run with different variational parameters, this corresponds to running a batch of circuits with each run of the quantum computer. This samples $p \times$ more data points from the energy landscape of the problem with every run. Together with a classical optimiser that makes best use of the batched circuits, this approach could also reduce the running time of the algorithm.

- Each parallel circuit could run an entire instance of VQE, with the results over all p instances either averaged at the end of the computation, or the minimum over all of them taken. This is equivalent to running the VQE algorithm p times, and could provide more certainty that the algorithm has succeeded if many of the parallel results agree.
- Each circuit could be used to measure a different term in the Hamiltonian as it is often not possible to calculate the expectation of the entire Hamiltonian in one circuit preparation. The speedup here will depend on how many groupings of Pauli terms there are, but it could also be combined with any of the methods above. This is what was done in [4, 6], combined with using different parameters. However, the available speedup for the Hubbard model from parallelising measurements alone would be relatively limited, as the energy can be measured using 5 measurements for an arbitrary lattice [12].

In this paper we focus on the first two forms of parallelism. For the remainder of this section, we will outline the different aspects of the VQE algorithm such as ansatz circuit, optimiser and the error mitigation techniques that need to be employed on the device.

We make use of the Hamiltonian variational (HV) ansatz [13] which has previously been shown to be effective for solving the Hubbard model in simulation [12–14] and in experiment [7, 8]. Each layer of the ansatz circuit consists of time-evolutions according to each of the terms in the Hamiltonian. The variational parameters govern the length of the time-evolution and the same parameter may be used for terms in the Hamiltonian that commute.

The 2×1 Hubbard model has a single hopping term and onsite term, therefore the ansatz has only two variational parameters per layer. Furthermore, numerical experiments have shown that only one layer of the ansatz is required to produce the ground state [12], making the full circuit that we run:

$$|\psi\rangle = e^{i\theta H_{\text{hop}}} e^{i\phi H_{\text{os}}} |\psi_0\rangle, \quad (2)$$

where $|\psi_0\rangle$ is the ground state of H_C with $U = 0$ (which can be prepared efficiently using Givens rotations [15]). Finally, to measure $\langle H_C \rangle$ requires two preparations of the quantum circuit as the onsite terms are measured in the computational basis and the hopping terms in the X basis. Figure 1 demonstrates this circuit in the Rigetti native gate set.

We use two different classical optimisation techniques in our experiments, each suited to a different form of parallelism. Both optimisation algorithms have been covered in detail elsewhere; we will restrict the discussion to their uses within parallel VQE.

The first optimiser is simultaneous perturbation stochastic approximation (SPSA) [16, 17] which has previously been used on small VQE experiments on superconducting quantum hardware [7, 18]. The SPSA algorithm works similarly to standard gradient descent, but

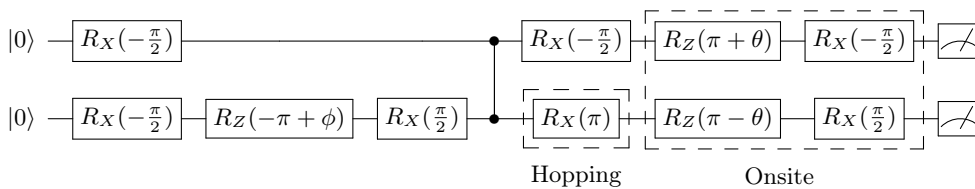


FIG. 1. Optimised quantum circuit (compiled for Rigetti hardware) to implement initial state preparation, one layer of the HV ansatz, and measurement of the Hamiltonian terms in H_C . The dashed boxes indicate gates that are included in the circuit when measuring the hopping or onsite terms. The circuit for measuring the hopping terms has a lower depth as the addition of the Hadamard gates for transforming into the X -basis has the effect of cancelling many of the R_X and R_Z rotations. In particular, R_Z gates (including those that depend on the hopping parameter θ) are moved to the end of the circuit where they do not have an effect on the computational basis measurements.

instead picks a random direction to estimate the gradient along. Each gradient evaluation is then estimated from two function evaluations, resulting in less calls to the quantum computer compared to other finite difference methods. We use SPSA with the first method of parallelism – running the same circuit with the same parameters in parallel.

The second optimiser we try is Bayesian model gradient descent (BayesMGD) which has been successfully used to solve the Hubbard model on 8 sites (16 qubits) using VQE on Google’s quantum hardware [8]. The idea behind BayesMGD is to sample points θ_i in a trust region around θ . A quadratic function is fitted to these points and used to approximate the gradient at θ , which is then used to perform gradient descent. A natural way of making use of this algorithm in parallel is to run each different point θ_i in parallel. One iteration of BayesMGD will then correspond to one run of the quantum computer.

Finally, we employ two simple error mitigation techniques in our experiments, noise inversion (NI) [19–21] and training with fermionic linear optics (TFLO) [22].

NI is a common technique designed to handle readout errors on small circuits. Before running VQE, we sample the readout noise by producing each computational basis state and measuring the outcome. We use this to construct a noise matrix \mathcal{N} where the elements at (i, j) are the estimated probability of measuring $|i\rangle$ given that we have prepared $|j\rangle$. If the measured probability distribution after running the VQE circuit is \tilde{d} , we can obtain an estimate of the ideal distribution using $d \approx \mathcal{N}^{-1}\tilde{d}$. Since the size of \mathcal{N} scales exponentially with the number of qubits, we apply it only locally to each pair of qubits in our parallel computation.

TFLO is a method for mitigating errors in quantum circuits that simulate fermionic systems [22]. Expectations of certain observables produced by fermionic linear optics (FLO) circuits can be computed exactly classically. If these FLO circuits approximate the circuits that we want to run on the quantum computer, the exact and approximate FLO results can be used to estimate the effect of errors in our non-FLO circuit. More concretely, in our case, the only non-FLO operation is the onsite evolution term. If we remove this term (i.e. set $\phi = 0$) then we have a suitable circuit for TFLO. We apply TFLO separately

to each pair of qubits at the end of the VQE algorithm using the simplest method presented in [22]. Suppose that we wish to estimate the energy $E(\phi, \theta)$ and the result we receive from the quantum computer is $\tilde{E}(\phi, \theta)$. We can correct the energy estimate using one TFLO data point as follows:

$$\tilde{E}(\phi, \theta) \mapsto \tilde{E}(\phi, \theta) + E(0, \theta) - \tilde{E}(0, \theta). \quad (3)$$

II. EXPERIMENTAL RESULTS

The device that all of the experiments in this paper are run on is the 80-qubit Rigetti Aspen-M-1 which allows for potentially 40 circuits to be run in parallel; the greatest number of parallel circuits that we report on is 33. In this section we will present experimental benchmarking and VQE results for running parallel two-qubit circuits.

A. Benchmarking and selection of qubit pairs

In order to determine which qubit pairs are usable, how they perform in parallel and how to best select them, it is necessary to do some benchmarking of the device. One simple experiment that can be done before running circuits in parallel is to run the two-qubit circuit on every possible pair individually and observe their performance. The purpose of this is to determine if the reported two-qubit gate fidelities are a good way of selecting qubit pairs, and also which error mitigation techniques are most effective.

The VQE framework allows for the use of the measured energy as a straightforward benchmark (the closer to the ground energy, the better). In a larger experiment where the ground energy and the corresponding VQE parameters are unknown, a heuristic that we have found to be effective is to use arbitrary parameters and assume that the lower the energy, the better. Although it is possible for errors to produce a lower energy state (perhaps by moving out of the given number sector into one that has a lower ground energy), in practice we have found that errors produce higher energy measurements when we ignore error correction. This is especially the case for

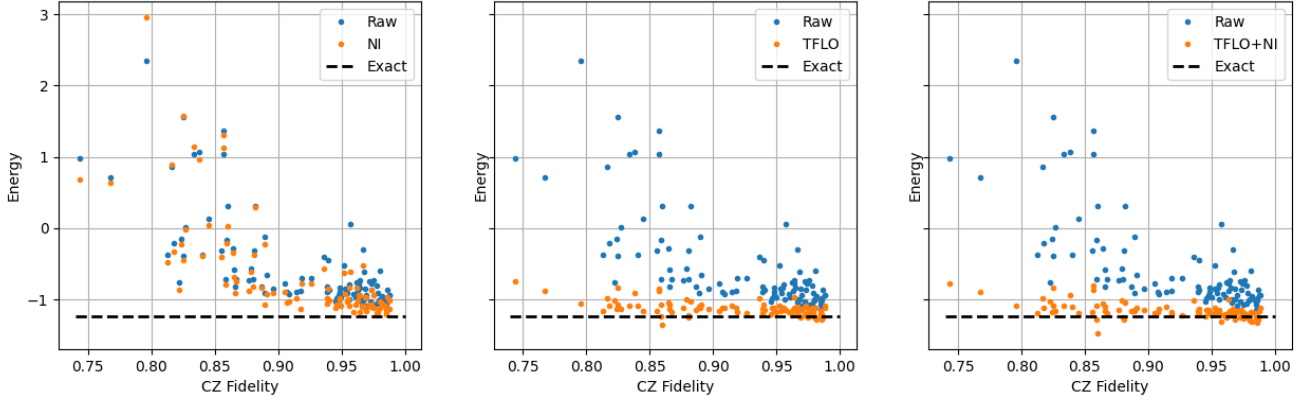


FIG. 2. Plot of reported CZ fidelity (from the Rigetti QCS website) against the energy obtained from running the optimal parameter VQE circuit. Circuits were run on each pair individually on Aspen-M-1 and the three graphs demonstrate the performance of different error mitigation techniques – Raw (no error correction), NI, TFLO and combined TFLO+NI. The optimal parameter and TFLO circuits were run on each pair using 10,000 shots.

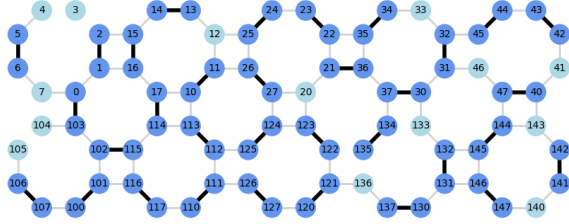


FIG. 3. Aspen-M-1 chip with 33 two-qubit circuits run in parallel. Connections are shown between qubits where it is possible to do a CZ gate, with the chosen pairs highlighted in bold.

arbitrary parameters achieving a relatively low energy as in general errors make the state more mixed, and the maximally mixed state has high energy.

Figure 2 is a plot of the reported CZ fidelity against the energy obtained by running the optimal parameter VQE circuit on all 97 pairs on Aspen-M-1. Qubit pairs that have a CZ fidelity of above 90% typically behave in a similar manner and perform well even without error mitigation, making these pairs a good choice for further experiments. However, the TFLO method of error mitigation brings the lower fidelity pairs in line with the higher fidelity pairs, meaning that it may be possible to use a larger part of the device for the parallel computations.

One way of making full use of the quantum computer is to use a maximum-weight perfect matching graph algorithm based on a graph of the device connectivity and reported CZ fidelities. For the Aspen-M-1 device, such an algorithm selects 39 pairs as missing connections on the device do not allow use of all 80 qubits. Although the perfect matching algorithm makes maximum use of the qubits on the device, it may be preferable to use a smaller, but more carefully selected, number of qubits. Through-

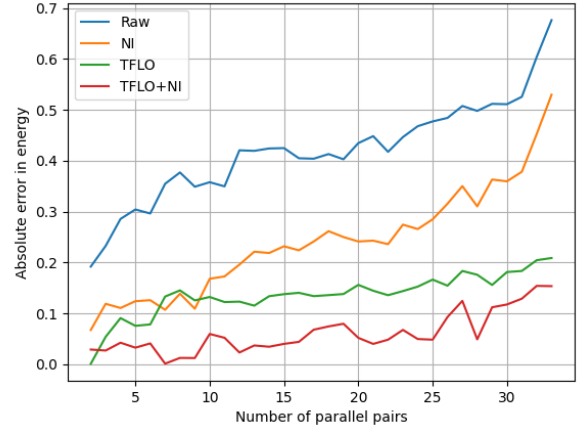


FIG. 4. The average absolute error with exact energy for qubit pairs in parallel for one run on Aspen-M-1. The optimal parameter circuit was run using 10,000 shots in parallel up to 33 pairs using greedy pair selection.

out this work we use a “greedy” method of selecting pairs where we pick the pair with the best CZ fidelity, remove that pair from the list of qubits, and repeat. This greedy pair selection typically selects a maximum of 33 pairs on Aspen-M-1 (an example of this is demonstrated in Figure 3), but is more flexible as we can pick how many pairs we want to select, or which CZ fidelity to cap the pair selection at.

In Figure 4 we put greedy pair selection in practice up to 33 pairs by running the same circuit and averaging the expectation of $\langle H_C \rangle$. The average error gets worse as more pairs are added, but by using TFLO, the error stays low up to 20-25 pairs. This behaviour seems to be due to the fact that we are adding pairs with worse fidelities rather than other factors such as crosstalk – see

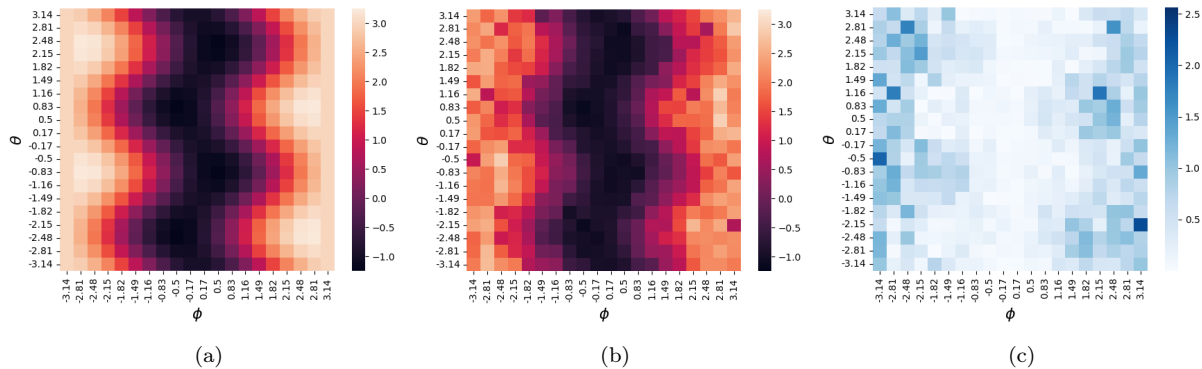


FIG. 5. Heatmap of the energy landscape for 20 points between $-\pi$ and π for the onsite and hopping parameters ϕ and θ , and taking 10,000 shots for each point. a) The exact energy landscape. b) On Aspen-M-1 using 25 pairs in parallel, 16 runs of the quantum computer and applying TFLO+NI for error mitigation. The running time for producing the heatmap was 3 minutes 40 seconds (this is doubled if we also run TFLO). In comparison, this would take 66 minutes to run if we only used one pair. c) The absolute error between the heatmaps a) and b).

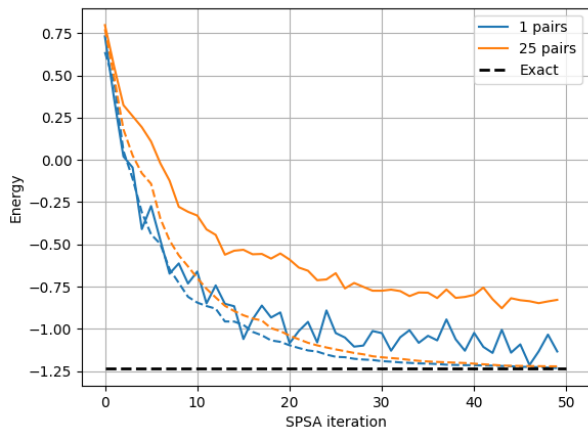


FIG. 6. Comparison of SPSA in parallel (using 25 pairs for one run on Aspen-M-1) and not in parallel using 1,000 shots to estimate the energy and NI applied throughout the optimisation. The dashed lines are the exact energy at the parameters given by SPSA, showing that the optimisation procedure on the quantum computer has found the optimal parameters, but the calculated energy needs correcting.

Figure 9 in the Appendix for a more detailed analysis. For larger and longer circuits, crosstalk will likely play a more dominant role [23], and the selection of the groups of qubits will need to take this into account [4].

B. Performance of parallel VQE

Since there are only two variational parameters ϕ and θ in the ansatz, we can generate a heatmap as an intuitive visual representation of the energy landscape. Figure 5 shows a heatmap containing 400 points that was

produced using only 16 runs of the quantum computer by running 25 pairs in parallel, leading to a speedup in running time of $18\times$ compared to one individual circuit. The key features of the energy landscape are reproduced in the parallel run. This means that we could rapidly generate a heatmap in parallel and then use information about where the minimum is to start a separate, more accurate, VQE optimisation closer to the optimal parameters. This may not scale to more variational parameters as the energy of more and more points would need to be estimated to get an overview of the energy landscape. However, it is possible a version of this where random points are sampled from the parameter space and used to direct a finer VQE optimisation could benefit from parallelisation.

For the rest of the experiments, we implement the full VQE algorithm. First, we present the results for SPSA where the form of parallelism that is used is running the same circuit on every pair and taking their average for the energy estimate. The SPSA metaparameters we use are $\alpha = 0.602$, $\gamma = 0.101$, $a = 0.15$, $c = 0.2$ from detailed numerical experiments conducted in [12]. Unlike in [12], we run only the one-stage SPSA algorithm (i.e. we do not change the number of shots taken throughout the optimisation) and set $A = 1$ as reducing this stability constant has been shown to be more effective in experiment [7, 8].

In Figure 6, we compare running SPSA with one pair and 25 pairs using 1,000 shots (see Figure 10 in the Appendix for the justification why we have chosen to do 1,000 shots). Both are able to find the optimal parameters, but although running parallel circuits has the effect of “smoothing out” the optimisation, similarly to Figure 4 the calculated energy is more of an overestimate. Another drawback from parallelisation here is the running time, the VQE algorithm took 245 seconds to run using one pair, but 420 seconds using 25 pairs; a greater overhead is introduced when more data is being passed back and forth between the quantum computer and the

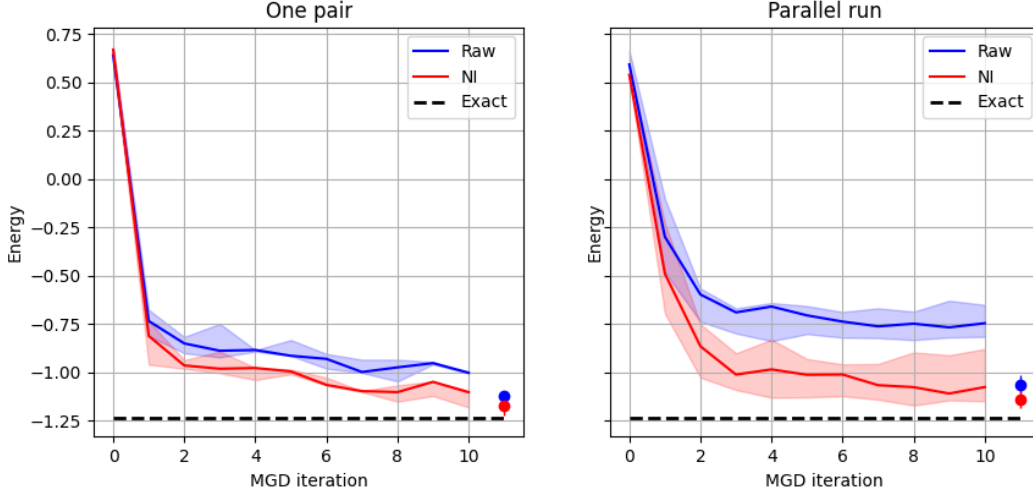


FIG. 7. Running BayesMGD on Aspen-M-1 on one pair and in parallel using 12 pairs, and 1,000 shots to estimate the expectation value. For the parallel run, one BayesMGD iteration provides 12 points of data in the trust region around θ . To compare the performance of the algorithm, we also take 12 points for each BayesMGD iteration during the individual run (equivalent to setting the metaparameter $\eta = 2$). The graphs show the median of 5 repetitions of the experiment for the parallel run and 4 for the individual run, the shaded region shows the minimum and maximum values of the energy reached. The dots show the final result after TFLO is applied, the minimum error reached for one pair was 0.0127, and for the 12 pairs was 0.0541. On average the running time of the individual run was 180 seconds, and 30 seconds for the parallel run.

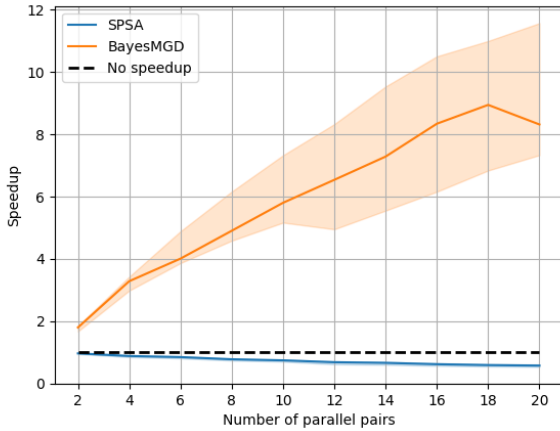


FIG. 8. Speedup in running time of parallel VQE using SPSA and BayesMGD. Line shows the median of 4 (5) repetitions when running SPSA (BayesMGD) in parallel, with the shaded region showing the minimum and maximum speedup.

classical computer.

Although SPSA works with parallel circuits, we do not appear to get a benefit from parallelisation of the same circuit. Another approach to take is to run the parallel circuits with different variational parameters, we do this with the BayesMGD optimiser. The metaparameters we use are $\alpha = 0.602$, $\delta = 0.6$, $\xi = 0.101$, $l = 0.2$ from [8], and $\gamma = 0.6$, $A = 1$ for moving through the parameter space faster. In our parallel VQE experiments, we do

not need to include the metaparameter η which governs the number of points θ_i in each iteration of BayesMGD. Instead, the number of points will be governed by the number of pairs we run in parallel. Figure 7 compares BayesMGD using 12 parallel circuits and one individual circuit. The graph shows that the parallel run roughly follows the individual run, and when TFLO is applied the results are comparable in quality. Note that an ideal running time speedup in this case would be $12\times$, here we achieve a $6\times$ speedup.

In these experiments, we have shown that it is possible to perform a full VQE computation using parallel circuits. For parallelisation to potentially be of use on NISQ hardware, we need to demonstrate a speedup taking into account all overheads. Figure 8 shows the speedup in wall-clock time with the number of pairs in parallel (see Figure 11 in the Appendix for the data showing performance against number of pairs). For BayesMGD recall that as the number of pairs increases, the corresponding algorithm on one pair makes more function evaluations. For SPSA, we are consistently doing 1,000 shots on every pair, so we do not expect to see a speedup. Ideally we would see an accuracy increase as the number of pairs increases, but this is not the case as we show in Figure 6 and 11.

III. CONCLUSION

In this paper we have demonstrated a minimal two-qubit parallel VQE example, running up to 33 circuits in

parallel for benchmarking and up to 25 circuits for the VQE algorithm. We selected a small two-qubit circuit that has already performed well on Rigetti hardware [7] to maximise the possibility for parallelisation given the restricted size of current quantum hardware. While we have demonstrated it is possible to conduct a full VQE experiment with parallel computations on the same quantum device (see Figure 6 and 7), there remain significant challenges for scaling up to larger circuits.

Although it is difficult to pin down the exact behaviours of the qubit pairs in parallel and individually, a general strategy that produced good results was to select pairs that had the best reported gate fidelities in the provided hardware statistics and prioritising quality over quantity. While the problem of finding suitable pairs can be solved using a matching algorithm or a greedy search, doing larger computations involves the more complicated problem of finding sub-graphs on the quantum device where the qubits are good quality and have the desired connectivity. A number of papers have proposed algorithms for doing this whilst taking account of the device specifications and crosstalk [3–6], and experiments have been conducted on IBMQ devices running up to four five-qubit computations in parallel [4].

In our experiments as we added more circuits in parallel, the accuracy of the results got worse as every pair being added had a worse fidelity, similarly to the findings of other investigations [3, 5]. This meant that the approach where the same circuit was run in parallel with the aim of producing more accurate results did not benefit from parallelisation. In fact, running one pair with a low number of shots was more accurate and had a shorter running time. For optimisation algorithms such as SPSA which are fairly sequential and do not require a lot of function calls per iteration, this would likely be the method of parallelisation to use, but it would not provide a benefit speed or accuracy wise.

The approach of running different circuits in parallel with the aim of gaining more information about the energy landscape sped up the runtime of heatmap generation and BayesMGD. Despite qubits of worse fidelity being included in the computation, we were able to produce good quality results (see Figure 5 and 7). It is likely that this method of parallelisation will work well with other optimisation algorithms that batch function evaluations such as evolutionary algorithms, or enable faster calculations of gradients using finite differences.

With methods such as these, the trade-off between speed and accuracy will need to be considered. For current quantum devices, due to low gate fidelities, one of the best uses of parallelism may be to carry out rough calculations such as the heatmap in Figure 5 and use the results to inform a more accurate VQE run on one circuit. For larger circuits and higher number of parameters, investigation is required to determine what types of useful rough calculations can be done. For example, this could involve determining the initial VQE parameters by randomly sampling from the parameter space; or rapidly

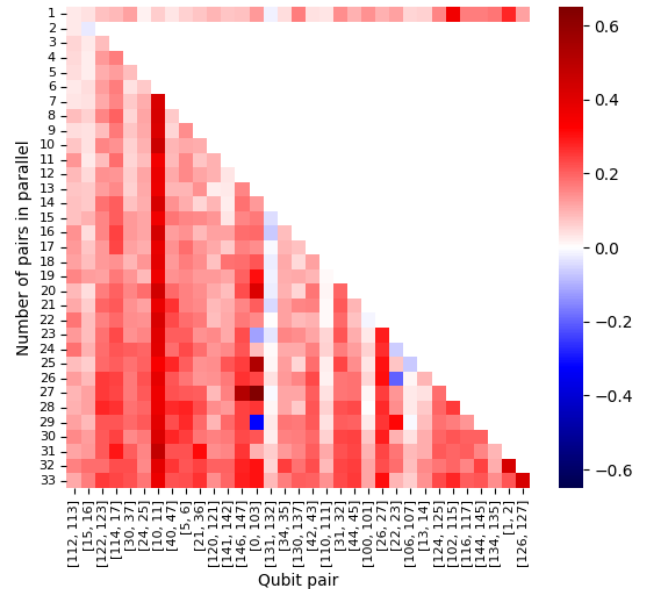


FIG. 9. Error with exact energy for qubit pairs in parallel on Aspen-M-1. The optimal parameter circuit was run using 10,000 shots in parallel up to 33 pairs using greedy pair selection, and also individually on each of these pairs. This graph shows the calculated energy (after TFLO was applied) minus the exact energy, for each qubit pair individually (top row) and for each parallel run it was included in. See Figure 3 for a visual representation of the 33 selected pairs.

building up a picture of a small but interesting region of the energy landscape. Overall, parallelisation could help to reduce the running time of VQE and the number of VQE optimisation steps required on NISQ devices.

ACKNOWLEDGEMENTS

We would like to thank other Phasecraft team members for their feedback on this work, and Rigetti for the access to their Aspen-M-1 hardware. This work was supported by Innovate UK (grant no. 44167) and has received funding from the European Research Council (ERC) under the European Union’s Horizon 2020 research and innovation programme (grant no. 817581).

Appendix A: Additional results

In this appendix we present additional results obtained from Aspen-M-1 over the course of the experiments carried out in Section II.

In Figure 4 we ran the same circuit in parallel using greedy pair selection up to 33 pairs. In Figure 9 we present the full data from this experiment by showing how each pair behaves in parallel and individually. The aim of this is to see if any systematic errors were intro-

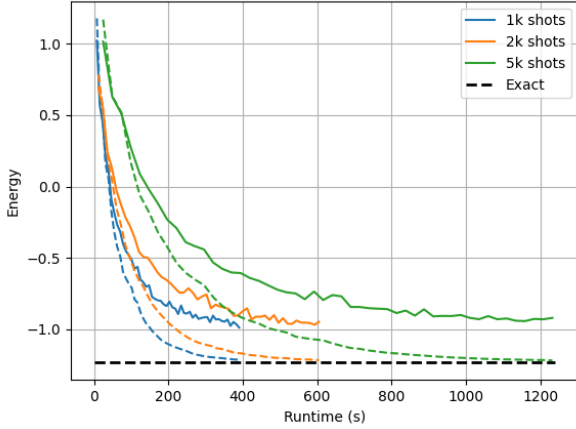


FIG. 10. Running SPSA on Aspen-M-1 using 26 pairs in parallel, using different numbers of shots to estimate the energy. For each of the runs, 50 SPSA iterations were done (corresponding to 150 circuit evaluations as SPSA requires two points to estimate the gradient, and we have also evaluated the circuit at θ to track the optimisation process) and NI was applied during the run. The dashed lines are the exact energy at the parameters given by SPSA.

duced in the results once more pairs were added. Note that only the last 7 pairs had a CZ fidelity below 90%. From Figure 4 we saw that the average error gets worse as more pairs are added, but TFLO still manages to keep the error lower up to 20-25 pairs. From Figure 9, this behaviour seems to be due to the fact that we are adding pairs with worse fidelities rather than crosstalk – for example, the performance of the two best pairs stay fairly consistent throughout the parallel runs.

On the other hand, it can be difficult to predict exactly how a pair will behave individually or in parallel – for example, pairs [10, 11] and [26, 27] perform well individually, but consistently overestimate the energy when in parallel. The Aspen-M-1 device is also formed from two 40-qubit devices with inter-chip connections placed between the two rows of octagons [24]. The pair [114, 17] is much more stable than [0, 103] in parallel whose performance fluctuates the most out of all of the other pairs; but both (and other inter-chip connections) have been observed to behave similarly to any other pair when running circuits individually.

Moving onto the VQE experiments, Figure 10 shows the results from running SPSA with parallel circuits (26 pairs were chosen using a greedy pair selection capped at 90% fidelity). In our benchmarking experiments in Section II A we fixed the number of shots at 10,000, here we show that SPSA performs well even using 1,000 shots. This allows us to fix 1,000 shots for all further VQE experiments.

Finally, in Figure 11 we present the full data from the SPSA and BayesMGD runs carried out in Figure 8. For SPSA, adding pairs does not change the underlying behaviour of the optimisation algorithm, instead we are effectively estimating the energy with more shots. However, as we have already seen, this does not improve the accuracy of the energy estimate; in fact, it makes it worse as we are adding in more shots from pairs with worse fidelities. With BayesMGD, we are effectively increasing the metaparameter η as we add more pairs, changing the underlying behaviour of the optimisation algorithm. In [8], the optimal value of η was 1.5 which corresponds to using 9 pairs in parallel. Below 8 pairs, the different BayesMGD runs in Figure 11 show a lot of variation, likely because the algorithm is not as effective for a low value of η . Above this, BayesMGD outperforms SPSA.

-
- [1] M. Cerezo, A. Arrasmith, R. Babbush, S. C. Benjamin, S. Endo, K. Fujii, J. R. McClean, K. Mitarai, X. Yuan, L. Cincio, and P. J. Coles. [Variational quantum algorithms](#). *Nat. Rev. Phys.*, 3(9):625–644, August 2021.
 - [2] K. Bharti, A. Cervera-Lierta, T. H. Kyaw, T. Haug, S. Alperin-Lea, A. Anand, M. Degroote, H. Heimonen, J. S. Kottmann, T. Menke, W.-K. Mok, S. Sim, L.-C. Kwek, and A. Aspuru-Guzik. [Noisy intermediate-scale quantum algorithms](#). *Reviews of Modern Physics*, 94(1):015004, February 2022.
 - [3] P. Das, S. S. Tannu, P. J. Nair, and M. Qureshi. [A case for multi-programming quantum computers](#). In *Proceedings of the 52nd Annual IEEE/ACM International Symposium on Microarchitecture*. ACM, 2019.
 - [4] S. Niu and A. Todri-Sanial. [Enabling multi-programming mechanism for quantum computing in the NISQ era](#). *Quantum*, 7:925, 2023.
 - [5] L. Liu and X. Dou. [QuCloud: A new qubit mapping mechanism for multi-programming quantum computing in cloud environment](#). In *2021 IEEE International Symposium on High-Performance Computer Architecture (HPCA)*. IEEE, 2021.
 - [6] S. Niu and A. Todri-Sanial. [How parallel circuit execution can be useful for NISQ computing?](#), 2021. arXiv:2112.00387.
 - [7] A. Montanaro and S. Stanisic. [Compressed variational quantum eigensolver for the Fermi-Hubbard model](#), 2020. arXiv:2006.01179.
 - [8] S. Stanisic, J. L. Bosse, F. M. Gambetta, R. A. Santos, W. Mruczkiewicz, T. E. O’Brien, E. Ostby, and A. Montanaro. [Observing ground-state properties of the Fermi-Hubbard model using a scalable algorithm on a quantum computer](#). *Nature Communications*, 13(1), 2022.
 - [9] J. Hubbard. [Electron correlations in narrow energy bands](#). *Proceedings of the Royal Society of London. Series A*, 276(1365):238–257, 1963.
 - [10] J. LeBlanc, A. E. Antipov, F. Becca, I. W. Bulik, G. K.-L. Chan, C.-M. Chung, Y. Deng, M. Ferrero, T. M. Henderson, C. A. Jiménez-Hoyos, E. Kozik, X.-W. Liu, A. J. Millis, N. Prokof’ev, M. Qin, G. E. Scuseria, H. Shi,

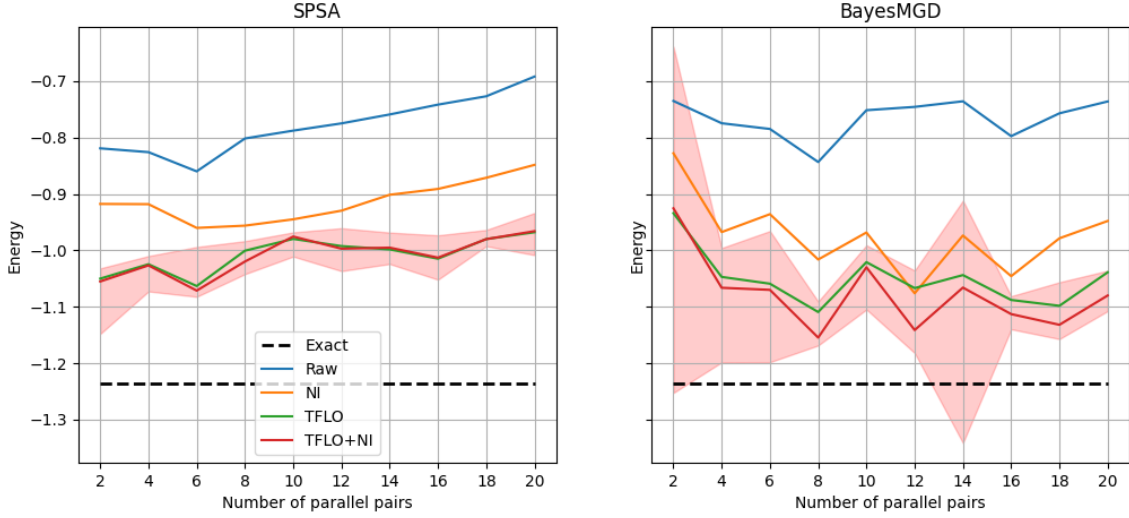


FIG. 11. Performance of SPSA and BayesMGD in parallel for different numbers of pairs and using 1,000 shots on Aspen-M-1. For each number of parallel pairs, we ran SPSA (capped at 20 iterations, with NI applied during the optimisation) 4 times, and BayesMGD (capped at 10 iterations) 5 times – this is due to the SPSA running time being much longer. The lines on the graphs show the median of the final results from the runs. For the TFLO+NI corrected (red) line, we also plot the minimum and maximum result reached.

- B. Svistunov, L. F. Tocchio, I. Tupitsyn, S. R. White, S. Zhang, B.-X. Zheng, Z. Zhu, and E. G. and. [Solutions of the Two-Dimensional Hubbard Model: Benchmarks and Results from a Wide Range of Numerical Algorithms](#). *Physical Review X*, 5(4):041041, 2015.
- [11] E. Dagotto. [Correlated electrons in high-temperature superconductors](#). *Reviews of Modern Physics*, 66(3):763–840, 1994.
- [12] C. Cade, L. Mineh, A. Montanaro, and S. Stanisic. [Strategies for solving the Fermi-Hubbard model on near-term quantum computers](#). *Physical Review B*, 102(23):235122, 2020.
- [13] D. Wecker, M. B. Hastings, and M. Troyer. [Progress towards practical quantum variational algorithms](#). *Phys. Rev. A*, 92(4):042303, 2015.
- [14] J.-M. Reiner, F. Wilhelm-Mauch, G. Schön, and M. Marthaler. [Finding the ground state of the hubbard model by variational methods on a quantum computer with gate errors](#). *Quantum Science and Technology*, 4(3):035005, 2019.
- [15] Z. Jiang, K. J. Sung, K. Kechedzhi, V. N. Smelyanskiy, and S. Boixo. [Quantum Algorithms to Simulate Many-Body Physics of Correlated Fermions](#). *Physical Review Applied*, 9(4), 2018.
- [16] J. C. Spall. [An overview of the simultaneous perturbation method for efficient optimization](#). *Johns Hopkins APL Technical Digest*, 19(4), 1998.
- [17] J. Spall. [Implementation of the simultaneous perturbation algorithm for stochastic optimization](#). *IEEE Transactions on Aerospace and Electronic Systems*, 34(3):817–823, 1998.
- [18] A. Kandala, A. Mezzacapo, K. Temme, M. Takita, M. Brink, J. M. Chow, and J. M. Gambetta. [Hardware-efficient variational quantum eigensolver for small molecules and quantum magnets](#). *Nature*, 549(7671):242–246, 2017.
- [19] S. Endo, S. C. Benjamin, and Y. Li. [Practical quantum error mitigation for near-future applications](#). *Physical Review X*, 8(3), 2018.
- [20] F. B. Maciejewski, Z. Zimborás, and M. Oszmaniec. [Mitigation of readout noise in near-term quantum devices by classical post-processing based on detector tomography](#). *Quantum*, 4:257, 2020.
- [21] S. Bravyi, S. Sheldon, A. Kandala, D. C. McKay, and J. M. Gambetta. [Mitigating measurement errors in multi-qubit experiments](#). *Physical Review A*, 103(4):042605, 2021.
- [22] A. Montanaro and S. Stanisic. [Error mitigation by training with fermionic linear optics](#), 2021. arXiv:2102.02120.
- [23] A. Ash-Saki, M. Alam, and S. Ghosh. [Experimental characterization, modeling, and analysis of crosstalk in a quantum computer](#). *IEEE Transactions on Quantum Engineering*, 1:1–6, 2020.
- [24] <https://www.globenewswire.com/news-release/2021/12/15/2352647/0/en/Rigetti-Computing-Announces-Next-Generation-40Q-and-80Q-Quantum-Systems.html>.